Analysis and Simplification of Kinetic Models for Methane Chlorination and Pyrolysis

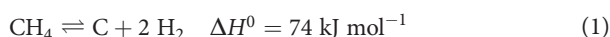**Florian Keuchel*, Moritz Heinlein, Jan Hohlmann, and David W. Agar**

So far, no complete reaction mechanism has been proposed for high temperature chlorination and pyrolysis of methane. Various mechanisms for the description of this reaction pathway are combined and compared in this paper. This adaptation shows that the gas phase pyrolysis of methane and methyl chloride can be combined with surface reactions via nucleation from the gas phase or on the reactor wall to reproduce the product spectrum. In addition, kinetic parameters for a global simplified one-step mechanism focused on the formation of carbon are fitted to available experimental data.

1 Introduction

Methane is a widely used chemical feedstock and fuel due to its energy content and excellent availability through existing infrastructure. Methane chlorination is used industrially for the production of chloromethanes, usually at temperatures up to 500 °C. If the chlorination is carried out at higher temperatures of over 1000 °C, a different product range is obtained, as intermediates begin to pyrolyze, while polycyclic aromatic compounds can be formed by the combination of radical species. In addition to the different products, the reaction enthalpy released at a high temperature level can also be exploited, being utilized in process integration to support other reactions or to generate electricity [1]. In this case, the motivation for the high temperature chlorination of methane (Eq. (2)) is to simultaneously pyrolyze excess methane (Eq. (1)) in the same reactor to produce hydrogen.

$$CH_4 \rightleftharpoons C + 2\,H_2 \quad \Delta H^0 = 74\ \text{kJ mol}^{-1} \tag{1}$$

$$CH_4 + 2\,Cl_2 \rightleftharpoons C + 4\,HCl \quad \Delta H^0 = -294\ \text{kJ mol}^{-1} \tag{2}$$

Through specially designed flow arrangements, carbon deposits on the reactor wall may also be avoided, which could overcome one of the key challenges facing endothermic methane pyrolysis [2, 3]. The heat released by the chlorination of a single methane molecule is much larger than that required for its pyrolysis. Methane can therefore be supplied in excess to leverage hydrogen production. The product sought is hydrogen, although solid carbon and hydrogen chloride may also be utilized in the overall integrated process. Chlorinated hydrocarbon compounds can impede the separation process, contaminate the carbon product and diminish hydrogen selectivity, therefore their formation as final products should be minimized.

The reaction pathway of methane chlorination can be modeled using a numerical approach. Gas phase reactions of both chlorination and pyrolysis occur, as well as solid formation by nucleation from the gas phase or at the reactor wall. The focus of this kinetic investigation for the chlorination reaction is directed towards the formation of carbon, since solid carbon can be regarded as an indicator of the completed reaction. By understanding the reaction network kinetics, reactors can be properly designed and unwanted by-products minimized. Fig. 1 depicts an overview of the various stages of the reaction.

Due to the high reaction temperatures, hydrogen is split off from methane giving rise to methyl radicals, which recombine to form C_2 species. These can be further dehydrogenated to yield radical acetylene and subsequently form aromatics by recombination. New radicals, especially radical acetylene, can then be added to the aromatics converting them into polycyclic aromatic hydrocarbons (PAHs; hydrogen-abstraction and C_2H_2-addition, HACA mechanism). When PAHs collide, nucleated particles are formed, which can subsequently aggregate. At their surface, other PAHs, as well as radical species, can further react, resulting in primary soot particles. The primary particles can then coagulate and adhere to the reactor walls. In the process, the coagulated particles are rounded off by surface growth. Thereafter, the particles begin to form agglomerates with a fractal structure. Carbon formation can also proceed via a

Florian Keuchel, Moritz Heinlein, Jan Hohlmann, Prof. Dr. David W. Agar
florian.keuchel@tu-dortmund.de
Technische Universität Dortmund, Fakultät Bio- und Chemieingenieurwesen/Lehrstuhl für Chemische Verfahrenstechnik, Emil-Figge-Strasse 66, 44227 Dortmund, Germany.
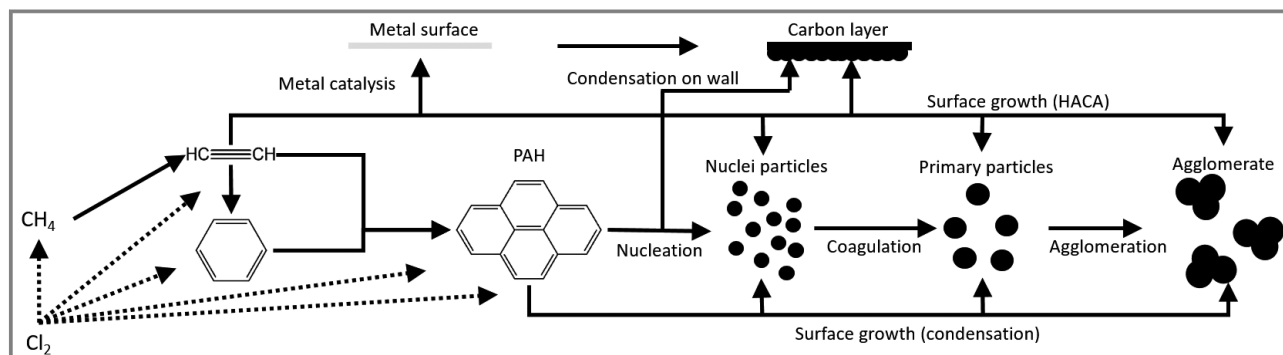
Figure 1. Reaction diagram of the various mechanisms for the pyrolysis of methane to carbon agglomerates, including the influence of chlorine [4–9].

metal-catalyzed route through the bonding of the radicals to the surface of a metal catalyst, so that a carbon layer grows on it. Chlorine acts as an accelerator and has a major influence on the formation of methyl radicals. In this case, the chlorine radicals react with the hydrogen atoms of the hydrocarbons, including those with high carbon numbers, and further radicals can be formed. Tran and Senkan found that the coke from methyl chloride pyrolysis does not contain any chlorine, so it is assumed that the solid products in this work are free of chlorine [4–9].

Hardly any experimental or kinetic data or complete mechanisms for this high-temperature methane chlorination at around 1000°C or higher are available in the literature. By combining different reaction mechanisms and fitting kinetic parameters to experimental data, new models are developed here to describe the pertinant reactions.

2 Modeling

The reactions were simulated using CHEMKIN 19.1 and MATLAB R2018a. The simulations in CHEMKIN were employed to investigate the combination of different mechanisms, by comparing, large reaction networks with one another and incorporating both gas phase and surface growth reactions. The studies conducted in MATLAB were used to simplify the mechanisms and only include gas phase reactions.

Isothermal behavior is assumed, since usually only a single specific temperature is given in the experimental data sets. Furthermore, one-dimensional reactors are used for modeling purposes. The reactor dimensions were adjusted to the conditions of the experimental measurements under consideration. The rate constants k are represented by the modified Arrhenius equation in Eq. (3), in which T describes the absolute temperature with the temperature exponent n, A is the pre-exponential factor and E_A is the activation energy.

$$k = AT^n \exp\left(-\frac{E_A}{RT}\right) \qquad (3)$$

If no rate constants for the reverse reactions were available, the equilibrium constants, as the ratios between forward and reverse reactions, were employed to determine them. For this purpose, the values of the free Gibbs energy and thus the enthalpy and entropy data were calculated via the corresponding NASA polynomials. Surface reactions were considered to be irreversible in this work, since none of the thermodynamic data for surface species is given to enable the calculation of the equilibrium constants.

The particles grow as a result of surface reactions and thus increase their surface area and consequently the number of reactive sites on the surface. Moreover, the particles can also collide, which can lead to coagulation. Accordingly, in order to calculate the surface area, information about the particle size distribution must be known. This was introduced via the method of moments, in a technique also used by Frenklach in the context of soot formation [4]. Agglomeration of the particles is not considered in this work, corresponding to its omission in that of Skjøth-Rasmussen et al., as this phenomenon occurs late on in the process and its inclusion significantly complicates the model [10].

3 Examination and Combination of Kinetic Models

First, the gas phase mechanism for methane pyrolysis was selected. Secondly, it is augmented by various surface mechanisms and the results are compared with experimental data. According to Fau et al., the gas phase mechanism of Sinaki is the most suitable for the description of methane pyrolysis, since it offers both good accuracy and an acceptable computational effort [11, 12].

For the modeling of the particle formation, the mechanism selected is extended by a surface reaction mechanism. Here, that of Wang and Frenklach (WF-SM) is the most obvious candidate. The Sinaki mechanism is based on the gas-phase mechanism of Appel et al., which in turn is an improvement upon the gas-phase mechanism of Wang and Frenklach, for which the WF-SM was developed [4, 13, 14]. The WF-SM is used with the extensions of Skjøth-Rasmussen et al. [10].

Using these mechanisms, however, the calculated carbon selectivity is only marginally above zero over the time interval considered. A possible explanation for this is that particle formation is too low when based only on this surface mechanism. Previously, the formation of carbon was described solely by nucleation in the gas phase. However, Blekkan et al. found that by performing the experiments for 10 min, a carbon layer was formed on the reactor wall [15]. Surface reactions could thus take place on both the wall and also on the particle surface. Therefore, ethylene could already have reacted to form further carbon before PAHs were formed. In CHEMKIN, this problem can be resolved qualitatively by assuming that the reactor wall is completely coated with carbon, on the surface of which the same reactions can occur as on the particle surfaces. Another reason is that particle formation starts earlier than that of pyrene. This is illustrated, for example, in the surface mechanism of Agafonov et al. (A-SM), which is why this mechanism was also considered in the simulation [16]. To verify the wall influence and the A-SM, Fig. 2 shows the comparison of the experimental values of Blekkan et al. with those obtained from the selectivities calculated with the A-SM and WF-SM with and without wall influence [15]. The wall influence was included by adding the surface area of the reactor as an additional area for all surface reactions, apart from the nu-

cleation reactions. In Fig. 2, it can be seen that the selectivities for ethylene and carbon, which are crucial for the surface mechanism, are best described by the A-SM. The experimental selectivities lie between the limiting cases without wall influence and with the wall completely coated with carbon.

Although this comparison suggests that the A-SM is the most suitable, this model was derived from a mechanism for shock tube experiments. The same mechanisms were therefore also compared for verification purposes with the experiments of Lucas et al. [17]. In the experiments shown in Fig. 3, methane was introduced into a 1 m long glass tube with a diameter of 22 mm at 1030 °C to 1092 °C. The differences within the five experiments in the data of Lucas et al. are mainly due to different temperatures, volume flows and reaction times. Here, it can be observed that the simulated concentrations are much more sensitive to such changes than the experimental data suggests. In this comparison too, illustrating the selectivities of hydrogen and carbon, the A-SM is again the most suitable option. It was thus chosen as the surface mechanism for methane pyrolysis and used together with the Sinaki mechanism for the gas-phase.

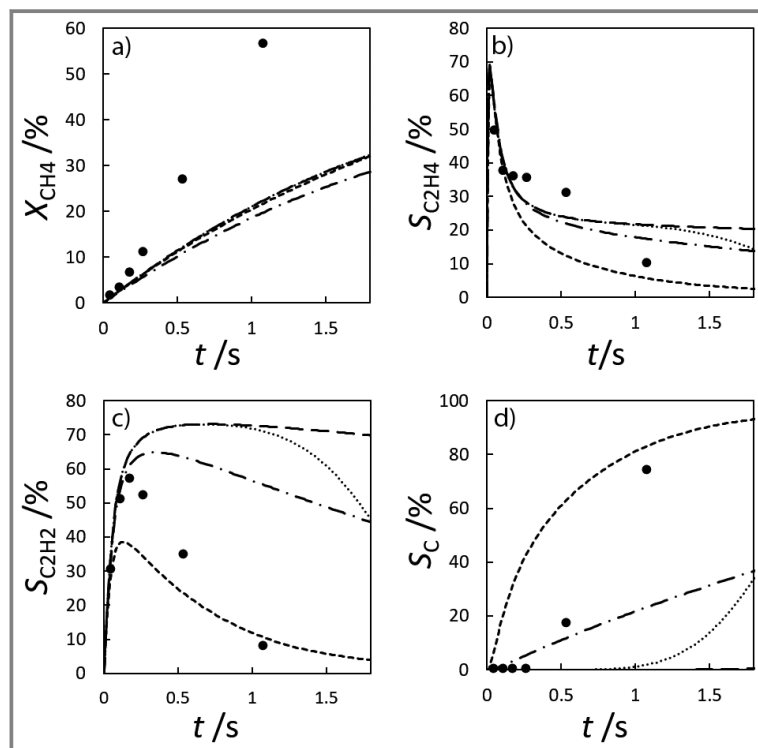Compared to methane pyrolysis, studies of methane chlorination offer only a few mechanisms involving the formation of carbon. Most reaction pathways only consider species up to C_2 or just describe the pyrolysis of chloromethanes. In this work, the mechanism of Mitchell et al. was chosen as the mechanism describing PAH formation in most detail [18]. Since it only represents the reactions up to naphthalene, while carbon formation often arises from larger PAHs, it was extended with the reactions of the Sinaki gas-phase mechanism, so that, for example, the surface mechanism of Wang and Frenklach becomes applicable. In the case of identical reactions and thermodynamic data, the values of Sinaki were used, reflecting their more recent origins. The combination of these two mechanisms results in the Mitchell-Sinaki mechanism (MS-M) devised in this work. This modification is compared to the original Mitchell-Mechanism (M-M) using the experimental values of Tavakoli et al., which are shown in Fig. 4 [19]. However, its use of above 1500 K data is uncertain due to the questionable validity of the thermodynamic data in this range.

Essentially, the experimental data are well reproduced by both mechanisms. Only minor differences between the original M-M and the merged MS-M can be observed. Thus, the MS-M can be used as the gas phase mechanism for further consideration.

Since, according to Tran and Senkan, there is no chlorine in the coke produced by the pyrolysis of methane with chlorine, and the chlorine
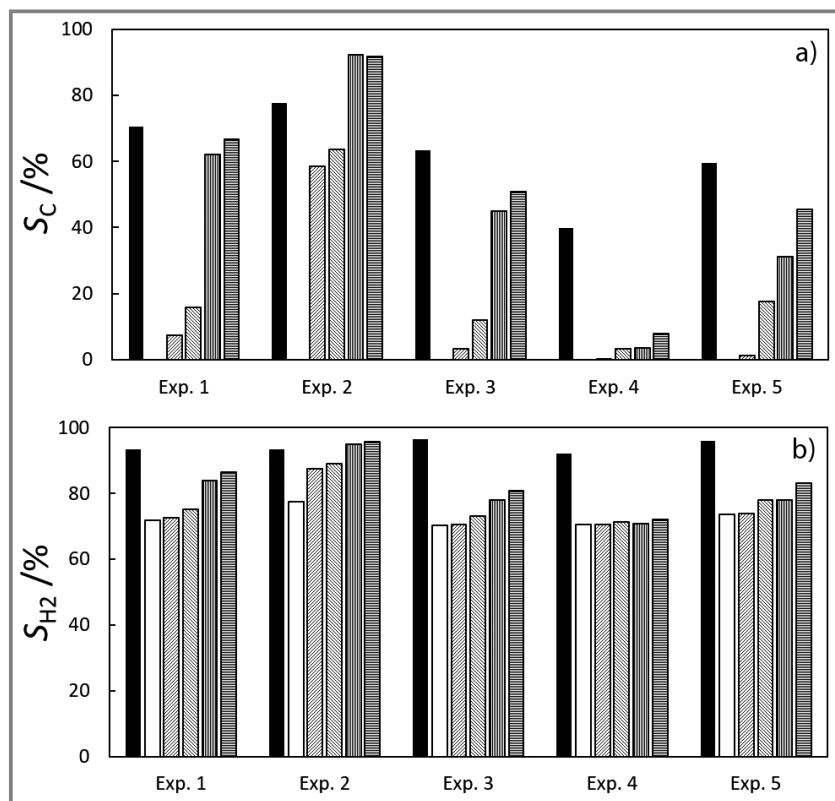

Figure 2. Effect of wall influence on various surface mechanisms at 1473 K. The simulated conversion of methane (a) and the selectivities of ethylene (b), acetylene (c), and carbon (d) using the WF-SM with (– · –) and without wall influence (– –) and the A-SM with (- - -) and without wall influence (···) are compared to experimental data (●) from Blekkan et al. [15].

www.cit-journal.com

© 2022 The Authors. Chemie Ingenieur Technik published by Wiley-VCH GmbH

Chem. Ing. Tech. **2022**, *94*, No. 5, 712–719

Figure 3. Comparison of the experimental values of Lucas et al. with various surface mechanisms with and without wall influence [17]. The selectivities of carbon (a) and hydrogen (b) based on the conversion of methane are presented. In addition to the experimental data by Lucas et al. (■), the data calculated for the gas-phase mechanism alone (□) are also given. The mechanisms used for the calculation are the WF-SM without wall influence (▨) and with wall influence (▧), and the A-SM and without wall influence (▥) and with wall influence (▤).
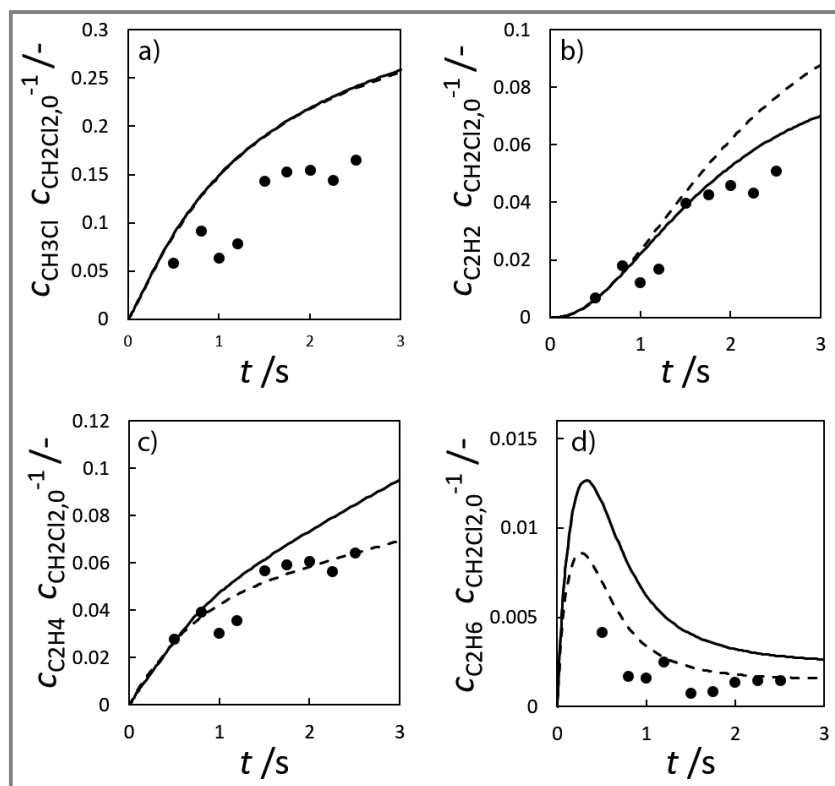

Figure 4. Comparison of chlorination mechanisms with experimental values of dichloromethane pyrolysis at 800 °C. The M-M (-) and the mechanism merged from those of Sinaki and Mitchell (- -) are compared with the results of Tavakoli et al. (●) using the normalized concentrations of methyl chloride (a), ethylene (b), acetylene (c) and ethane (d) [19].
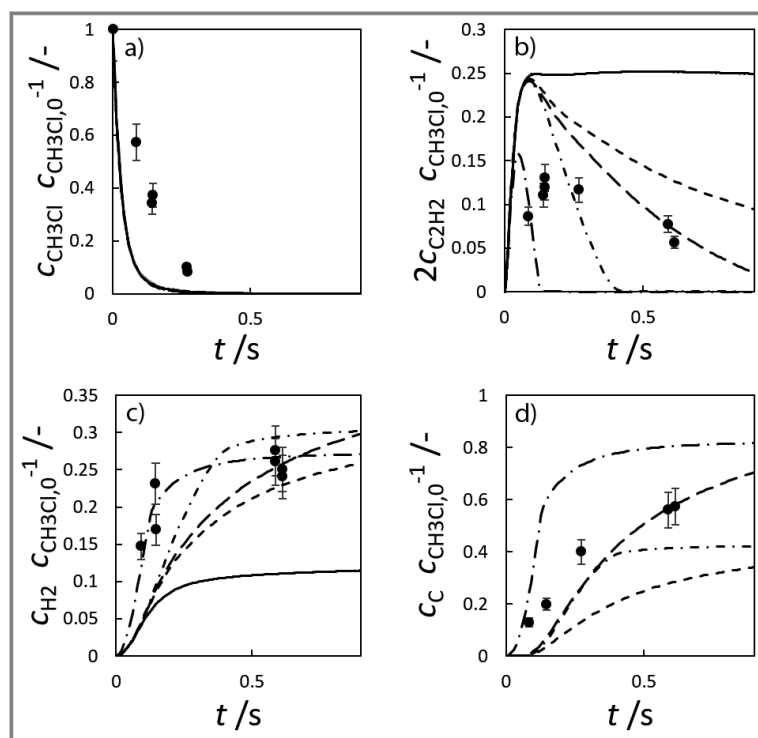
Figure 5. Comparison of the MS-M and the mod. MS-M with the A-SM on the basis of experimental data of the methyl chloride pyrolysis. The concentration curve of the substances methyl chloride (a), ethylene (b), hydrogen (c) and carbon (d) are normalized using the inlet concentration of methyl chloride. The experimental values (●) were determined by Weissman et al. at 1310 K and 369 Torr with an accuracy of 12% [9]. In addition to the data calculated with the MS-M with (– –) and without wall influence (- -), the data calculated with the mod. MS-M calculated data with the A-OM with (– · –) and without wall influence (- · ·), as well as the concentration curves calculated without surface mechanism of the MS-M (-) are shown.

radicals participate only in hydrogen splitting reactions, the same surface mechanisms as for methane pyrolysis should be applicable [8]. It is therefore assumed that the A-SM is also a suitable surface mechanism for methane chlorination. To verify this, the MS-M is compared with the experimental data of Weissman et al. for a methyl chloride pyrolysis as shown in Fig. 5 [9].

The low hydrogen and carbon concentrations and the overly high ethylene concentration could result from the fact that, due to the merging of the Mitchell mechanism with the Sinaki mechanism, the reactions proceeding from naphthalene are no longer included. The HACA mechanism for the PAH growth thus takes place more slowly, so that the ethylene concentration is too high and fewer particles are formed. To verify whether reactions with chlorine and PAHs beyond naphthalene have an effect on carbon selectivity, several of the reactions listed in Tab. 1 with the kinetic parameters given were added to the gas phase mechanism. The additional reactions are only those in which a hydrogen atom is split off by a chlorine radical, where the values were adopted according to the mechanism of Mitchell et al. [18].

In order to verify this new modified Mitchell-Sinaki mechanism (mod. MS-M), the reactions with and without wall influence are also compared in Fig. 4. Without the surface mechanism, the concentration curves obtained with MS-M and the mod. MS-M do not differ. With the surface mechanism on the other hand, the concentration of ethylene with the mod. MS-M deviates from the unmodified model. Without wall influence, the peak of the ethylene concentration is still overestimated, but the concentration drops much faster than in the experiment. The hydrogen concentration is slightly underestimated without wall influence at short residence times. With wall influence, the experimental concentrations can be matched more accurately.

From this comparison it can be concluded that the modification leads to a faster formation of carbon so that the experimental values can be found between the two limiting cases with and without wall influence, in contrast to the unmodified MS-M. The peak of ethylene is captured better, as is the concentration curve for hydrogen. For these reasons, the final mechanism used for chlorination is the mod. MS-M, with chlorine interactions up to pyrene, together with the A-SM, which was also extended to include the interaction with chlorine.

4 Simplification of Kinetic Models

The description of the reaction presented so far was carried out with mechanisms from larger reaction networks. Due to their complexity, however, these mechanisms are unsuitable for detailed flow simulations, since the computation times become excessive. Therefore, the goal of this section of the work was to create highly simplified kinetic models for methane chlorination and pyrolysis. These mechanisms will be compared with data from the literature for validation and subsequently optimized as appropriate.

Various multi-step mechanisms were created and compared with experimental data. The number of steps refers to the number of reaction equations describing the overall global reaction process. The largest set of experimental data is given by Weissman et al., who pyrolyzed pure methyl chloride and a mixture of methyl chloride and methane [9]. The temperature in the reactor was set at 1260 K or 1310 K and maintained as constant as possible, with a variation of between 2 K and 25 K (0.15–2 %). A total of 6 data sets with different system pressures and temperatures are available. This data is special in that the amount of carbon formed is given, as calculated via a mass balance. Particularly noticeable in the data of Weissman et al. are the variations of the results between the individual data sets. For example,

Table 1. Reaction equations added to the mechanisms. Here A_x describes the molecule of x aromatic rings. A_2, for example, is naphthalene. A_2R_5 is acenaphthylene. The suffix "–" or "*" points out that the molecule is a radical. The numbers after the "–" or the "A" and "B" in the product species of 7th to 9th reactions indicate different positions of the abstracted hydrogen. For all reactions in this table, the temperature exponent n is 0 and the pre-exponential factor A is $1.0 \cdot 10^{14}$ cm³mol⁻¹s⁻¹.

Reaction equation	E_A [cal mol⁻¹]
$A_2 + Cl \rightleftharpoons A_2 - 1 + HCl$	1100
$A_2 + Cl \rightleftharpoons A_2 - 2 + HCl$	1100
$A_3 + Cl \rightleftharpoons A_3 - 1 + HCl$	1100
$A_3 + Cl \rightleftharpoons A_3 - 4 + HCl$	1100
$A_2R_5 + Cl \rightleftharpoons A_2R_5 - + HCl$	1100
$A_4 + Cl \rightleftharpoons A_4 - + HCl$	1100
$A_2C_2H_2 + Cl \rightleftharpoons A_2C_2HA + HCl$	0
$A_2C_2HA + Cl \rightleftharpoons A_2C_2HA^* + HCl$	0
$A_2C_2HB + Cl \rightleftharpoons A_2C_2HB^* + HCl$	0
$H(S) + Cl \longrightarrow (S) + HCl$	1100
$Cl + A_1 \rightleftharpoons A_1 - + HCl$	1100
$Cl + C_6H_5CH_3 \rightleftharpoons C_6H_5CH_2 + HCl$	0

Table 2. Results of different simulation solutions for the one-step fitting mechanism in Eq. (4).

Solution	A [s⁻¹] *	n [–]	E_A [J mol⁻¹]
1	1.49	1.30	2.96
2	$3.68 \cdot 10^{12}$	1.05	$3.03 \cdot 10^5$
3	2.43	1.00	1.50

*depending on the reaction order

changing the pressure at 1310 K from 258 Torr to 271 Torr at constant temperature leads to a 50 % reduction of the hydrogen concentration and to 20 % less methyl chloride conversion. The influence of such deviations on the investigations presented must be treated with caution. The sum of the relative error squares between simulated and experimental data is chosen as the objective function to be minimized.

Since different multi-step mechanisms were to be tested, a 5-step mechanism was first created according to Benzinger's design [20]. Due to the very high computation times, even with the temperature exponent n set to 1, mechanisms with fewer reaction steps, i.e., 2, 3, and 4 steps, were devised. Several solutions were found for each of these mechanisms. In particular, the magnitudes of E_A can vary greatly. Since the different solutions resulted in very similar concentration curves and the lumping of different mechanisms proved unable to narrow down the magnitudes of the parameters, all multi-step mechanisms were discarded in favor of a simple 1-step mechanism. This was formulated according to the following simplified reaction (Eq. (4)).

$$CH_3Cl \longrightarrow C + H_2 + HCl \qquad (4)$$

Once again, the fitting is based on the amount of carbon formed, since this can be identified as a measure for the progress of the reaction and is of particular interest in possible flow simulations. Another advantage of fitting the amount of carbon is that by analyzing several data sets an averaging is performed. Different solutions for the 1-step mechanism are listed in Tab. 2.

The upper and lower limits of the pre-exponential factor and the activation energy were varied, since for the 1-step mechanism several solutions also led to very similar concentration profiles. The optimized objective function of relative errors lies in a narrow range in all cases, so that the inaccuracy of the experimental values themselves plays a greater role than the optimization algorithm. The result of the second data set, for example, can be compared, to the global methane pyrolysis mechanism from Keipi et al., which exhibited a pre-exponential factor of $8.5708 \cdot 10^{12}$ s⁻¹ and an activation energy of $3.37 \cdot 10^5$ J mol⁻¹. The reaction order is given as 1.123. The range of validity of the kinetic parameters is between 1070 K and 1450 K [21]. For n set to 1, the best fit is given in the third solution. Fig. 6 shows an example of two experimental data sets of Weissman compared to the third kinetic parameter set from Tab. 2.

In general, the simulated data shown indicate that the concentration curve is not visibly affected by temperature. At 369 Torr, the deviation between the results at 1260 K and 1310 K at $t = 1$ s is $5.4 \cdot 10^{-3}$ %. Since the kinetic parameters were fitted to the carbon concentration, the concentration of methyl chloride is overestimated. This was to be expected and is inherently related to the selection of the one-step mechanism, as no other species, such as ethylene, acetylene or benzene, are formed to which methyl chloride might react. This means that the concentrations of methyl chloride and carbon cannot be matched simultaneously using a one-step mechanism, because in experiments the methyl chloride concentration would decreases much faster than the carbon concentration increases.

5 Conclusion

In this work, several mechanisms for methane chlorination and pyrolysis are presented, compared and validated based on experimental data. For methane pyrolysis, the mechanism of Sinaki et al. is preferred as the gas-phase mechanism [17]. To determine the surface mechanism for methane pyrolysis, the mechanism of Wang and Frenklach was compared with the surface mechanism of Agafonov et al., with the approach of Agafonov being selected. The mechanism of Mitchell et al. is chosen as the basis of the gas-phase mechanism for methane chlorination, as it is designed for both the chlorination of methane and the formation of
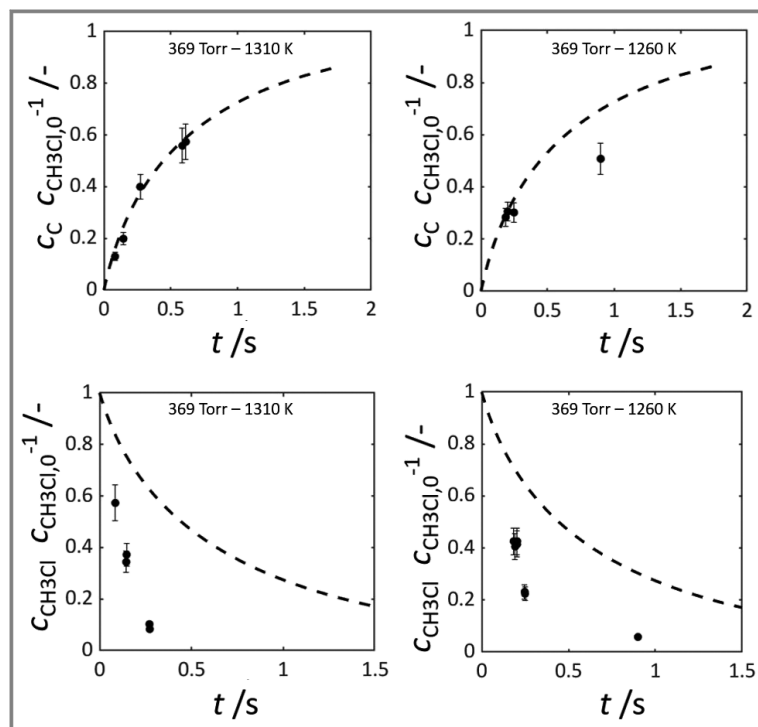
Figure 6. Comparison of the simulated data of the one-step mechanism with the different experimental data on carbon formation of Weissman et al. [9]. Kinetic parameters are the fitted parameters from run 3 of the optimization. Experimental data are shown as dots (●) and simulated data as dashed lines (- -). The measurement inaccuracy of 12% is indicated by error bars at the experimental data points.

Symbols used

A	$[m^x mol^{-y} s^{-1}]$	pre-exponential factor
c	$[mol\, m^{-3}]$	concentration
E_A	$[J\, mol^{-1}]$	activation energy
H	$[J\, mol^{-1}]$	reaction enthalpy
k	$[m^x mol^{-y} s^{-1}]$	reaction rate
n	$[-]$	temperature exponent
R	$[J\, mol^{-1} K^{-1}]$	gas constant
S	$[-]$	selectivity
t	$[s]$	time
T	$[K]$	temperature
X	$[-]$	conversion

Sub- and Superscripts

0	initial or standard condition

Abbreviations

A-SM	Agafonov surface mechanism
HACA	hydrogen-abstraction & C_2H_2-addition
M-M	Mitchell mechanism
Mod	modified
MS-M	Mitchell-Sinaki mechanism
PAH	polycyclic aromatic hydrocarbons
WF-SM	Wang and Frenklach surface mechanism

PAHs [18]. Since it describes only chain growth up to naphthalene, this mechanism is supplemented by reactions of Sinaki mechanism. The gas-phase mechanism, as well as the surface mechanism, are extended with reactions to describe the influence of chlorine beyond naphthalene. This leads to an improved accuracy in fitting the experimental results of Weissman et al. [9].

For fitting the kinetic parameters, no mechanism can be found that can adequately describe the concentration of both the reactant methyl chloride and the product carbon. However, a one-step mechanism can be adapted in such a way that it models the formation of carbon quantitatively well. Nevertheless, several solutions yielding similar concentration profiles were found. Since only one source of experimental data is available, it is not possible to say which of the values ascertained is actually correct. The comparison with literature sources is also not informative in this regard, as the values found for activation energies and pre-exponential factors also vary greatly. By generating further experimental data, a more differentiated and detailed analysis of the parameters obtained from the optimization would be possible, providing a reliable basis for reactor flow simulations.

References

[1] J. González Rebordinos, A. H. Salten, D. W. Agar, *Int. J. Hydrogen Energy* **2017**, *42 (7)*, 4710–4720. DOI: https://doi.org/10.1016/j.ijhydene.2016.09.071

[2] B. F. Latham, JR., *US Patent 3 377 137 A*, **1968**.

[3] T. Becker, F. Keuchel, D. W. Agar, *Chem. Ing. Tech.* **2021**, *93 (5)*, 762–770. DOI: https://doi.org/10.1002/cite.202000234

[4] M. Frenklach, H. Wang, in *Soot Formation in Combustion*, Vol. 59, Springer Series in Chemical Physics (Eds: V. I. Goldanskii et al.), Springer, Berlin **1994**.

[5] L. F. Albright, J. C. Marek, *Ind. Eng. Chem. Res.* **1988**, *27 (5)*, 755–759. DOI: https://doi.org/10.1021/ie00077a006

[6] I. Naydenova, M. Nullmeier, J. Warnatz, P. A. Vlasov, *Combust. Sci. Technol.* **2004**, *176 (10)*, 1667–1703. DOI: https://doi.org/10.1080/00102200490487544

[7] M. Frenklach, J. P. Hsu, D. L. Miller, R. A. Matula, *Combust. Flame* **1986**, *64 (2)*, 141–155. DOI: https://doi.org/10.1016/0010-2180(86)90051-9

[8] T. Tran, S. M. Senkan, *Ind. Eng. Chem. Res.* **1994**, *33 (1)*, 32–40. DOI: https://doi.org/10.1021/Ie00025A006

[9] M. Weissman, S. W. Benson, *Int. J. Chem. Kinet.* **1984**, *16 (4)*, 307–333. DOI: https://doi.org/10.1002/kin.550160403

[10] M. Skjøth-Rasmussen, P. Glarborg, M. Østberg, J. Johannessen, H. Livbjerg, A. Jensen, T. Christensen, *Combust. Flame* **2004**, *136 (1–2)*, 91–128. DOI: https://doi.org/10.1016/j.combust-flame.2003.09.011

[11] G. Fau, N. Gascoin, P. Gillard, J. Steelant, *J. Anal. Appl. Pyrolysis* **2013**, *104*, 1–9. DOI: https://doi.org/10.1016/j.jaap.2013.04.006

[12] M. Y. Sinaki, E. A. Matida, F. Hamdullahpur, *Int. J. Hydrogen Energy* **2011**, *36 (4)*, 2936–2944. DOI: https://doi.org/10.1016/j.ijhydene.2010.12.002

[13] J. Appel, H. Bockhorn, M. Frenklach, *Combust. Flame* **2000**, *121 (1–2)*, 122–136. DOI: https://doi.org/10.1016/S0010-2180(99)00135-2

[14] H. Wang, M. Frenklach, *Combust. Flame* **1997**, *110 (1–2)*, 173–221. DOI: https://doi.org/10.1016/S0010-2180(97)00068-0

[15] E. A. Blekkan, R. Myrstad, O. Olsvik, O. A. Rokstad, *Carbon* **1992**, *30 (4)*, 665–673. DOI: https://doi.org/10.1016/0008-6223(92)90186-Z

[16] G. L. Agafonov, A. A. Borisov, V. N. Smirnov, K. Y. Troshin, P. A. Vlasov, J. Warnatz, *Combust. Sci. Technol.* **2008**, *180 (10–11)*, 1876–1899. DOI: https://doi.org/10.1080/00102200802261423

[17] P. Lucas, A. Marchand, *Carbon* **1990**, *28 (1)*, 207–219. DOI: https://doi.org/10.1016/0008-6223(90)90115-F

[18] T. J. Mitchell, S. W. Benson, S. B. Karra, P. Donald, K. B. Loker, *Combust. Sci. Technol.* **1995**, *107 (4–6)*, 223–260. DOI: https://doi.org/10.1080/00102209508907807

[19] J. Tavakoli, J. A. Doney, *Chem. Eng. Commun.* **1993**, *119 (1)*, 135–150. DOI: https://doi.org/10.1080/00986449308936112

[20] W. Benzinger, A. Becker, K. J. Hüttinger, *Carbon* **1996**, *34 (8)*, 957–966. DOI: https://doi.org/10.1016/0008-6223(96)00010-3

[21] T. Keipi, T. Li, T. Løvås, H. Tolvanen, J. Konttinen, *Energy* **2017**, *135*, 823–832. DOI: https://doi.org/10.1016/j.energy.2017.06.176